

# Discovering two-dimensional magnetic topological insulators by machine learning

Haosheng Xu,<sup>1</sup> Yadong Jiang,<sup>1</sup> Huan Wang,<sup>1</sup> and Jing Wang<sup>1,2,3,\*</sup>

<sup>1</sup>State Key Laboratory of Surface Physics and Department of Physics, Fudan University, Shanghai 200433, China

<sup>2</sup>Institute for Nanoelectronic Devices and Quantum Computing,

Zhangjiang Fudan International Innovation Center, Fudan University, Shanghai 200433, China

<sup>3</sup>Hefei National Laboratory, Hefei 230088, China

(Dated: October 26, 2023)

Topological materials with unconventional properties have been investigated intensively for both fundamental and practical interests. Thousands of topological materials have been identified by symmetry-based analysis and *ab initio* calculations. However, the predicted magnetic topological insulators with genuine full band gaps are rare. Here we employ this database and supervisedly train neural networks to develop a heuristic chemical rule for electronic topology diagnosis. The learned rule is interpretable and diagnoses with a high accuracy whether a material is topological using only its chemical formula and Hubbard  $U$  parameter. We next evaluate the model performance in several different regimes of materials. Finally, we integrate machine-learned rule with *ab initio* calculations to high-throughput screen for magnetic topological insulators in 2D material database. We discover 6 new classes (15 materials) of Chern insulators, among which 4 classes (7 materials) have full band gaps and may motivate for experimental observation. We anticipate the machine-learned rule here can be used as a guiding principle for inverse design and discovery of new topological materials.

Topological materials are exotic states of matter characterized by topologically nontrivial electronic band structure [1–16]. Ever since the birth of the field, widespread efforts from first-principles calculations in synergy with topological band theory have been devoted to identify and catalogue candidate topological materials [17, 18]. The recent theoretical frameworks known as topological quantum chemistry [19–21] and symmetry indicators [22–24] enable efficient diagnosis of topological materials using only symmetry data of the wavefunction [25, 26]. These symmetry-based methods facilitate fruitful computational searches for topological materials [27–32]. However, certain forms of band topology and low-symmetry systems are invisible to symmetry indicators [22]. For example, Chern insulators and time-reversal invariant  $Z_2$  topological insulators (TI) without any point group symmetry cannot be diagnosed by symmetry indicators, and their topological nature can be determined only by evaluating the wavefunction-based topological invariant directly, which requires significant computational cost. Moreover, the complicated magnetic structure of materials hinders diagnosis by using magnetic topological quantum chemistry [31]. Thus, for practical reason, it is highly desirable to develop broadly applicable rules to determine whether a given electronic material is topological.

Recently, machine learning (ML) has become a novel efficient tool for predicting topological materials [33–38] and topological invariants [39–41]. Among these applications, a heuristic chemical rule for electronic topology diagnosis has been proposed, which does not depend on the crystal symmetry [38]. Motivated by understanding of chemical bonding from electronegativity as its tendency to attract electrons, they termed a ML numerical value for each element as *topogivity*, which loosely captures its

tendency to form topological materials. The heuristic rule for electronic topology of a given material is determined by the sign of weighted average of its elements' topogivities. New non-symmetry-diagnosable topological materials have been predicted by the heuristic rule and density functional theory (DFT) validation. In spite of these successes, their work only involved non-magnetic materials and did not include many transition metal elements which constitute magnetic materials. From the perspective of first-principles calculation, the topology of magnetic materials may depend on Hubbard  $U$  parameters [31]. Thus the dependence of topology on  $U$  value cannot be captured by their chemical rule [38, 42–44]. Meanwhile, the number of confirmed magnetic topological materials is less than ten [45]. This motivate us to develop ML chemical rule for efficient electronic topology diagnosis and searches for magnetic materials.

Here, as illustrated in Fig. 1, we use the convolutional neural network (CNN) to search for chemical rules of topological electronic structure by including Hubbard  $U$  value. We obtain training parameters  $\tau_E$  (referred as topogivity) for each element in the periodic table, and find the heuristic rule of a given material is diagnosed with high accuracy (average 83.9%) as topologically nontrivial (trivial) if the weighted average of its elements' topogivities is positive (negative). Here the element weight of a given material is determined by both the element's fraction and Hubbard  $U$  parameter (Fig. 2). The convolution layers correctly capture the influence of  $U$  value on the topological properties of magnetic materials displayed in the training set. We first test our heuristic rule to predict non-symmetry-diagnosable and non-magnetic topological materials as in Ref. [38] and get very similar accurate results. Then we proceed to perform model evaluation in Chern insulators [46–63], and find our heuristic rule

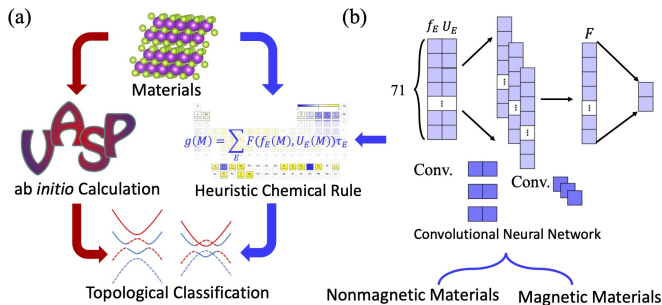


FIG. 1. Heuristic chemical rule diagnosis and DFT discovery of topological materials. (a) The topogivity-based heuristic diagnosis of a given material is evaluated by weighting the material’s elements’ topogivities  $\tau_E$  with  $\mathcal{F}(f_E, U_E)$ , where  $\mathcal{F}(f_E, U_E)$  is determined by element’s fraction  $f_E$  in the chemical formula and Hubbard parameter  $U_E$ . The high-throughput search for topological materials is performed by rapid heuristic rule screening through the material database to get candidate topological materials, and then followed by DFT calculations [65]. (b) Schematic of the ML workflow and structure of CNN, where the heuristic chemical rule is learned with both non-magnetic and magnetic materials as input.

for diagnosis still has a high balanced accuracy  $\sim 82.8\%$  (Fig. 3). Finally, we integrate ML rule with DFT calculations to search for magnetic TI in 2D MatPedia [64], and find T-phase  $\text{RuO}_2$ ,  $\text{OsO}_2$ ,  $\text{GdBr}$  and  $\text{TbX}$  family are new Chern insulators with full band gaps.

**Training and testing dataset.** We employ a supervised learning to obtain heuristic chemical rule for topological materials diagnosis. Here the training dataset consists of nonmagnetic and magnetic, stoichiometric, three-dimensional materials, where we label TIs, topological crystalline insulators and topological semimetals (TSM) as topological materials, and refer all other materials as trivial materials. The nonmagnetic dataset utilizes a subset of the database developed in Ref. [29], where only the space groups with nontrivial symmetry indicator groups are taken [66]. We add the data of magnetic materials identified in Ref. [31], where the same material with transition metal element of different  $U$  values may belong to different topological classifications. For instance,  $\text{Mn}_5\text{Si}_3$  is a TI with  $U = 0$  for Mn, a TSM with  $U = 1$  eV, and trivial with  $U = 2, 3, 4$  eV. Here we consider a given magnetic material with different Hubbard  $U$  parameters as different inputs, which further expands our magnetic training data (see Supplementary Material for methodology of constructing the training dataset). Then our labeled dataset comprises 9284 materials, of which 51.8% are marked as topological (69.5% are TSM) and the remaining 48.2% are marked as trivial. However, it is worth noting that certain topology may not be correctly identified by symmetry-based methods, thus the training dataset should be viewed as a set with noisy labels. The evaluation of our model is performed in several different settings which are not contained in training dataset.

**Heuristic chemical rule and CNN.** Our ML heuristic chemical rule takes the form

$$g(M) = \sum_E \mathcal{F}(f_E(M), U_E(M)) \tau_E, \quad (1)$$

where the summation runs over all elements in material  $M$ ,  $\tau_E$  is a learned parameter for element  $E$ , and  $\mathcal{F}$  is learned by the convolution layers (Fig. 2), which is a function of  $f_E(M)$  and  $U_E(M)$ . Here  $f_E(M)$  is the element fraction for element  $E$  in material  $M$  (e.g., for a chemical formula  $X_a Y_b Z_c$ ,  $f_X(M) = \frac{a}{a+b+c}$ ,  $f_Y(M) = \frac{b}{a+b+c}$ ,  $f_Z(M) = \frac{c}{a+b+c}$ ), and  $U_E(M)$  is Hubbard  $U$  value for element  $E$  (if the element is non-magnetic, we set it to zero). The sign of  $g(M)$  decides the classification: classify as topological (trivial) if  $g$  is positive (negative). A larger value of  $g(M)$  roughly corresponds to a more confident classification decision. Thus a diagnosis is obtained only by material’s chemical formula and Hubbard  $U$  parameters.

The structure of CNN is shown in Fig. 1(b). A material is described by a  $71 \times 2$  matrix with each row representing an element of periodic table. The first and second columns represent the element’s fraction and  $U$  value of the material, respectively. The convolutional network has two convolutional layers with 3 kernels of size  $1 \times 2$  and 1 kernel of size  $1 \times 1$ , followed by a binary classification neural network. The total number of trainable parameters is 151. All the hidden layers have rectified linear units  $\text{relu}(x) = \max\{0, x\}$  as activation functions. The output layer has softmax activation function given by the shape of  $(\frac{e^A}{e^A + e^B}, \frac{e^B}{e^A + e^B})^T$ , where  $A = \sum_E \mathcal{F}_E a_E$  and  $B = \sum_E \mathcal{F}_E b_E$ . The model is trained by marking trivial material as  $(1, 0)^T$  and topological material as  $(0, 1)^T$ . The network produces two sets of learning parameters  $a_E$  and  $b_E$  for each element  $E$ , we find the material is judged to be topological when  $\frac{e^B}{e^A + e^B} > \frac{e^A}{e^A + e^B}$ , which is equivalent to  $B - A = \sum_E \mathcal{F}_E (b_E - a_E) \equiv \sum_E \mathcal{F}_E \tau_E > 0$ .

It is interesting to compare our learned chemical rule to that learned by support vector machine in Ref. [38] which applies to non-magnetic materials only. For non-magnetic materials with  $U = 0$ ,  $\mathcal{F}(f_E(M), 0) \propto f_E(M)$ , then Eq. (1) reduces to  $g(M) \propto \sum_E f_E(M) \tau_E$ , which is exactly the same heuristic rule learned in Ref. [38]. While for magnetic elements with finite  $U$ ,  $\mathcal{F}$  is no longer a simple function of  $f_E(M)$ , and  $\mathcal{F}(f_E(M), U_E(M)) < \mathcal{F}(f_E(M), 0)$ , namely Hubbard  $U$  value reduces the weighting of corresponding magnetic element. Thus the topogivity  $\tau_E$  for each element  $E$ , loosely captures the tendency of an element to form topological materials.

We first evaluate our model performance within the labeled dataset before making predictions in different settings. We did eight-fold cross-validation and averaged the results over multiple test sets, and found an average of 83.9% accuracy. Moreover, we find empirically the fraction of accurately classified materials increases as the value of  $g(M)$  increases. The accuracy reaches 93% when

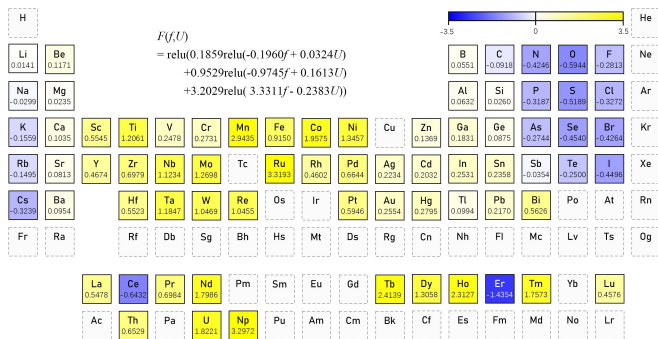


FIG. 2. Periodic table of ML topogivities  $\tau_E$  and combinatorial weight  $\mathcal{F}(f, U)$ .  $\tau_E$  are shown by color-coding and in values. Elements that appear less than 15 times in the labeled dataset are shown in gray with dashed box.

$|g(M)| \approx 3.5$ , after which the accuracy does not increase significantly [66]. Specifically, we observe on average that 94.8% of materials with  $g(M) \geq 4.0$  are correctly classified to be topologically nontrivial. Having completed the cross validation, we use the entire labeled dataset to fit the final model, which is what we will use for making predictions in different regimes. We observed the balanced accuracy for the magnetic materials only in the training dataset is 82.8%. Additionally, we found that the balanced accuracy of the model is better for materials with two or three distinct elements than for materials with one or four distinct elements.

Our model’s learned topogivities and weightings  $\mathcal{F}$  are shown in Fig. 2, where the elements that appear less than 15 times in the labeled dataset are shown in gray (see the full table of elements’ topogivities and appearing times in Supplementary Material). This table of topogivities enables a fast heuristic diagnosis of any stoichiometric material whose elements are featured in the periodic table. For example, magnetic TI  $\text{MnBi}_2\text{Te}_4$  [46, 67, 68] does not appear in the labeled dataset, Weyl semimetal TaAs [12, 13] is non-symmetry-diagnosable, but both of them are successfully diagnosed as topological by our learned rule:  $g(\text{MnBi}_2\text{Te}_4) = 1.195$  ( $U = 3$  eV for Mn) and  $g(\text{TaAs}) = 4.86$ .

The specific learned value of element topogivities are in general affected by the dataset and modeling limitations. However, several chemical heuristics can be extracted from the table of topogivities qualitatively. First, similar to Ref. [38], two clusters of elements located in the top right and bottom left parts of the periodic table have negative topogivities, which is consistent with intuition, since these two clusters tend to form ionic crystals and often have trivial band gaps. Second, considering groups 13 to 16, the topogivity decreases as one move from left to right across a period and increases as one move down a group, which is opposite to the electronegativity trend in the periodic table. This is also consistent with intuition that heavier elements have larger spin-

orbit coupling and weaker electronegativities form covalent crystals with smaller band gap, both of them often play important roles in topological materials. Finally, we observe all transition metals have positive topogivities. As Hubbard  $U$  increases, the weighting of transition metal elements decreases in a material, which leads to decreasing of  $g(M)$ . This is consistent with the intuition that large  $U$  value often lead to Mott insulator. Overall, these chemical insights suggest the topogivity-based picture and heuristic rule can provide a useful way to study topological materials.

*Evaluating the rule in different settings.* We then evaluate our model in different regimes of materials compared to the labeled dataset. First, we apply the learned rule and compute  $g(M)$  for materials in the discovery space, which contains 1431 non-symmetry-diagnosable and non-magnetic materials [38, 66]. We set a threshold of 1.6 for  $g(M)$  which corresponds to a high-confidence topological nontrivial classification, and leaves 79 materials. We further eliminate 7 materials which contain 4f or 5f electron with 72 materials left for DFT validation. We perform DFT within generalized-gradient approximation, and include spin-orbital coupling [66]. Of the 72 materials, we find 62 topological materials, corresponding to a success rate of 86.1%. All of the 62 topological materials are TSM, where 55 materials are consistent with the finding in Ref. [38]. Among the remaining 7 topological materials that we identified here, 3 have been predicted previously in the literature and the rest 4 represent truly new materials discovery [66].

Second, we use the final model to compute  $g(M)$  for trivial magnetic materials identified in Ref. [31]. There are 200 such materials (after the remove of 41 materials containing elements without topogivities) which are trivial at any  $U$  value. The test dataset is generated by combining these materials with different  $U$  values. We find that the model classifies 77.6% of materials in this set as trivial. It is interesting to compare this 77.6% number to the specificity, which is the fraction of samples classified as trivial among all the samples that have a label of trivial. We observe some deterioration in model performance, where the test specificity is  $85.6 \pm 1.6\%$  in the cross validation process.

At last, we evaluate our model performance to Chern insulators predicted by DFT calculations [46–63]. There are quite a few classes of 2D Chern insulator materials with full band gaps. For example, thin film of intrinsic magnetic TI family  $\text{Mn}_m\text{Bi}_{2n}\text{Te}_{m+3n}$  [46–50], FeI and TiTe [51–54], LaX [55, 56], transition metal trihalides  $\text{MX}_3$  [57–60], etc. The test dataset is generated by these materials with different  $U$  values [66], since the Chern insulators would be trivial under certain Hubbard  $U$  parameters from DFT. This individual dataset is heavily imbalanced in terms of the ratio of topological labels to trivial labels. The computed  $g(M)$  vs  $U$  for these 2D magnetic materials is shown in Fig. 3.  $g(M)$  is a de-

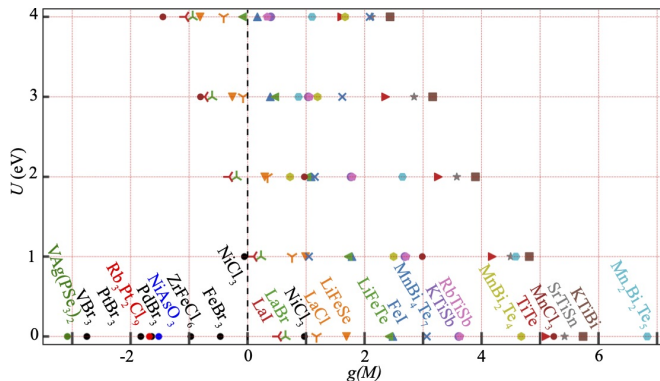


FIG. 3. The computed  $g(M)$  vs  $U$  for Chern insulators, which were predicted by first-principles calculations under certain Hubbard  $U$  parameters. Materials with  $g(M) < 0$  at  $U = 0$  is shown only, for they are even more negative at finite  $U$ .

creasing function of  $U$ , but not always monotonic. We find the balanced accuracy of our final model is 82.8%. We stress that the validation dataset and the labeled dataset correspond to different regimes of materials, and so it is quite interesting that a model that was fit on the labeled dataset of 3D materials still works in the validation dataset of 2D materials. Additionally, we observe the misclassification in  $\text{MX}_3$  and  $\text{Rb}_3\text{Pt}_2\text{Cl}_9$ , because the halogen with negative topogivities have a dominant fraction in the chemical formula, while their orbitals are far away from Fermi energy and do not contribute to topological bands.

*High throughput screening of 2D material and first-principles calculation.* Finally, we employ the topogivity-based chemical rule to identify 2D magnetic TI with genuine full band gaps, which are *extremely rare* in the literatures compared to 3D TSM and TI. We compute  $g(M)$  for each of 6351 2D materials from 2DMatPedia [64], and found 28% has positive  $g(M)$ . We focus our attention to materials that have a  $g(M) \geq 6$  value at  $U = 0$  that corresponds to a topologically nontrivial classification with high-confidence: that leaves 234 materials listed in Supplementary Materials. We then eliminate 137 materials without magnetic moment with 97 left for DFT validation. We find 16 magnetic topological materials, among which 11 are TSM [66] and the rest 5 ( $\text{TbX}$ ,  $\text{RuO}_2$ ) are new classes of Chern insulators listed in Table I. To our knowledge these have not been previously predicted. We also find topological band inversion with SOC induced gap in  $\text{TaCoTe}_2$ , which has been predicted and experimentally observed [69, 70]. Furthermore, we expand the search list and set a threshold of  $6 > g(M) \geq 0$ , and find 18 Chern insulators, where 8 have been predicted previously [66] shown in Fig. 3 and only  $\text{MnBi}_2\text{Te}_4$  has already been experimentally observed. The rest 10 are new material discovery listed in Table I, where  $\text{OsO}_2$  and  $\text{GdBr}$  have full band gap,  $\text{ScX}$  and  $\text{YX}$  are metallic but

Materials	2DMat id (2dm-)	$g(M)$	$\mathcal{C}$
$\text{TbX}$	959, 3600, 3487, 225	4.4, 4.1, 3.6, 3.5	-1
$\text{RuO}_2$	6443	2.5	2
$\text{OsO}_2$	3912	1.7	2
$\text{GdBr}$	5865	0.1	-1
$\text{ScX}$	1139, 3544, 1219, 1254	1.5, 1.2, 0.7, 0.6	-1
$\text{YX}$	984, 4695, 870, 3198	1.0, 0.7, 0.2, 0.1	-1

TABLE I. Newly discovered Chern insulators by the heuristic chemical rule and first-principles calculations.  $X = \text{F}, \text{Cl}, \text{Br}, \text{I}$ . Here  $g(M)$  is computed with  $U = 2, 4, 1, 0$  eV for Ru, Tb, Os, and Gd (Sc, Y), respectively. The first 4 classes have full band gaps, while the remaining 2 classes have Fermi pockets. The topogivities of Os and Gd are in Supplementary Materials.

have nontrivial Wilson loop [66].

We highlight two particularly interesting newly discovered Chern insulators in Fig. 4. Both of them have topological nontrivial full band gaps, making it promising for potential experimental investigation. T-phase  $\text{RuO}_2$  has a hexagonal lattice with space group  $P-3m1$  (No. 164). Its monolayer was predicted to be unstable and Peierls distorted into T'-phase [71]. However, recent experiment has observed stable T-phase  $\text{RuO}_2$  when fabricating H-phase  $\text{RuO}_2$  nanosheets [72]. The topology is from spin up band of  $d_{z^2}$  orbitals and spin down band of  $d_{xz, yz}$  orbitals of Ru at  $\Gamma$  point, which leads to  $\mathcal{C} = 2$ .  $\text{TbX}$  also form a hexagonal lattice with space group  $P-3m1$  (No. 164), the topology is from spin down band of  $d_{z^2}$

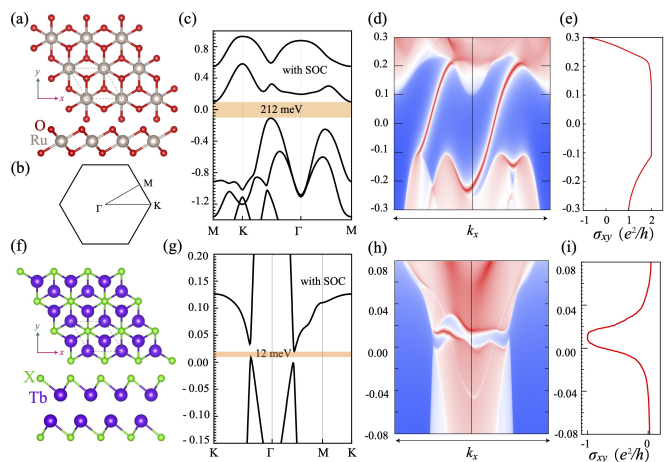


FIG. 4. Electronic structure and topological properties of monolayer  $\text{RuO}_2$  and  $\text{TbBr}$  by DFT+ $U$  ( $U=2, 4$  eV for Ru- $d$ , Tb- $f$  orbital, respectively). (a)-(e)  $\text{RuO}_2$ , (f)-(i)  $\text{TbBr}$ , The top and side views of atomic structure; the band structure with SOC; topological edge states calculated along  $x$  axis; anomalous Hall conductance  $\sigma_{xy}$  as a function of Fermi energy. (b) Brillouin zone. The shaded regions in (e) and (k) denote the topological gap.

orbitals and spin up band of  $d_{xy, x^2-y^2}$  orbitals of Tb at  $\Gamma$  point, and leads to  $\mathcal{C} = -1$ . Detailed analysis on topology of these two systems are in Supplementary Materials.

**Discussion.** The topogivity-based approximate picture of Eq. (1) provides a simple but coarse-grained approach for topological materials diagnosis with high accuracy, using only its chemical composition and Hubbard  $U$  value, without costly DFT calculations. Our final model cannot guarantee that a real material has topological features, which must be validated by DFT calculation. Still, it provides a fast and efficient tool to classify topological nature of a given material. The magnetic materials dataset helps us to get topogivity data on vast number of transition metal elements. We observe that materials in general with a large number of  $d$ - or  $f$ -shell valence electrons, and compounds containing heavy elements with strong spin-orbit coupling, have a greater tendency to be topological nontrivial.

Future research should try to take into account the relative electronegativity of the elements in the compounds. Many misclassified materials (with three or more distinct elements) have element taking a large fraction, but only acting as anion and not contributing to topological band around Fermi energy. Also it is necessity to verify the heuristic rule with more advanced graph neural network by taking materials' crystal symmetry into account. Then it is important to fully understand why the heuristic chemical rule here works so well, which may further elucidate the fundamental question of why some materials are topological while others are not. Furthermore, it is interesting to perform more comprehensive searches and inverse design for new magnetic topological materials using our learned model.

**Acknowledgment.** This work is supported by the National Key Research Program of China under Grant No. 2019YFA0308404, the Natural Science Foundation of China through Grant No. 12174066, the Innovation Program for Quantum Science and Technology through Grant No. 2021ZD0302600, Science and Technology Commission of Shanghai Municipality under Grant No. 20JC1415900, Shanghai Municipal Science and Technology Major Project under Grant No. 2019SHZDZX01.

---

\* Corresponding author: wjingphys@fudan.edu.cn

- [1] M. Z. Hasan and C. L. Kane, "Colloquium: Topological insulators," *Rev. Mod. Phys.* **82**, 3045–3067 (2010).
- [2] Xiao-Liang Qi and Shou-Cheng Zhang, "Topological insulators and superconductors," *Rev. Mod. Phys.* **83**, 1057–1110 (2011).
- [3] C. L. Kane and E. J. Mele, "Quantum Spin Hall Effect in Graphene," *Phys. Rev. Lett.* **95**, 226801 (2005).
- [4] B. Andrei Bernevig, Taylor L. Hughes, and Shou-Cheng Zhang, "Quantum spin hall effect and topological phase transition in hgte quantum wells," *Science* **314**, 1757–1761 (2006).
- [5] Markus König, Steffen Wiedmann, Christoph Brüne, Andreas Roth, Hartmut Buhmann, Laurens Molenkamp, Xiao-Liang Qi, and Shou-Cheng Zhang, "Quantum Spin Hall Insulator State in HgTe Quantum Wells," *Science* **318**, 766–770 (2007).
- [6] Liang Fu, C. L. Kane, and E. J. Mele, "Topological insulators in three dimensions," *Phys. Rev. Lett.* **98**, 106803 (2007).
- [7] Y. L. Chen, J. G. Analytis, J.-H. Chu, Z. K. Liu, S.-K. Mo, X. L. Qi, H. J. Zhang, D. H. Lu, X. Dai, Z. Fang, S. C. Zhang, I. R. Fisher, Z. Hussain, and Z.-X. Shen, "Experimental realization of a three-dimensional topological insulator, bi<sub>2</sub>te<sub>3</sub>," *Science* **325**, 178–181 (2009).
- [8] Liang Fu, "Topological crystalline insulators," *Phys. Rev. Lett.* **106**, 106802 (2011).
- [9] Yoichi Ando and Liang Fu, "Topological crystalline insulators and topological superconductors: From concepts to materials," *Ann. Rev. Condens. Mat. Phys.* **6**, 361–381 (2015).
- [10] Wladimir A. Benalcazar, B. Andrei Bernevig, and Taylor L. Hughes, "Quantized electric multipole insulators," *Science* **357**, 61–66 (2017).
- [11] Z. K. Liu, B. Zhou, Y. Zhang, Z. J. Wang, H. M. Weng, D. Prabhakaran, S.-K. Mo, Z. X. Shen, Z. Fang, X. Dai, Z. Hussain, and Y. L. Chen, "Discovery of a three-dimensional topological dirac semimetal, na<sub>3</sub>bi," *Science* **343**, 864–867 (2014).
- [12] Su-Yang Xu, Ilya Belopolski, Nasser Alidoust, Madhab Neupane, Guang Bian, Chenglong Zhang, Raman Sankar, Guoqing Chang, Zhujun Yuan, Chi-Cheng Lee, Shin-Ming Huang, Hao Zheng, Jie Ma, Daniel S. Sanchez, BaoKai Wang, Arun Bansil, Fangcheng Chou, Pavel P. Shibayev, Hsin Lin, Shuang Jia, and M. Zahid Hasan, "Discovery of a Weyl fermion semimetal and topological Fermi arcs," *Science* **349**, 613–617 (2015).
- [13] B. Q. Lv, H. M. Weng, B. B. Fu, X. P. Wang, H. Miao, J. Ma, P. Richard, X. C. Huang, L. X. Zhao, G. F. Chen, Z. Fang, X. Dai, T. Qian, and H. Ding, "Experimental Discovery of Weyl Semimetal TaAs," *Phys. Rev. X* **5**, 031013 (2015).
- [14] L. X. Yang, Z. K. Liu, Y. Sun, H. Peng, H. F. Yang, T. Zhang, B. Zhou, Y. Zhang, Y. F. Guo, M. Rahn, D. Prabhakaran, Z. Hussain, S. K. Mo, C. Felser, B. Yan, and Y. L. Chen, "Weyl semimetal phase in the non-centrosymmetric compound taas," *Nature Phys.* **11**, 728 (2015).
- [15] N. P. Armitage, E. J. Mele, and Ashvin Vishwanath, "Weyl and Dirac semimetals in three-dimensional solids," *Rev. Mod. Phys.* **90**, 015001 (2018).
- [16] Barry Bradlyn, Jennifer Cano, Zhijun Wang, M. G. Vergniory, C. Felser, R. J. Cava, and B. Andrei Bernevig, "Beyond Dirac and Weyl fermions: Unconventional quasiparticles in conventional crystals," *Science* **353**, aaf5037 (2016).
- [17] A. Bansil, Hsin Lin, and Tanmoy Das, "Colloquium: Topological band theory," *Rev. Mod. Phys.* **88**, 021004 (2016).
- [18] Jiewen Xiao and Binghai Yan, "First-principles calculations for topological quantum materials," *Nature Rev. Phys.* **3**, 283–297 (2021).
- [19] Barry Bradlyn, L Elcoro, Jennifer Cano, MG Vergniory, Zhijun Wang, C Felser, MI Aroyo, and B Andrei Bernevig, "Topological quantum chemistry," *Nature* **547**,

- 298 (2017).
- [20] Jorrit Kruthoff, Jan de Boer, Jasper van Wezel, Charles L. Kane, and Robert-Jan Slager, “Topological classification of crystalline insulators through band structure combinatorics,” *Phys. Rev. X* **7**, 041069 (2017).
- [21] Luis Elcoro, Benjamin J. Wieder, Zhida Song, Yuanfeng Xu, Barry Bradlyn, and B. Andrei Bernevig, “Magnetic topological quantum chemistry,” *Nature Communications* **12**, 5965 (2021).
- [22] Hoi Chun Po, Ashvin Vishwanath, and Haruki Watanabe, “Symmetry-based indicators of band topology in the 230 space groups,” *Nature Commun.* **8**, 50 (2017).
- [23] Haruki Watanabe, Hoi Chun Po, and Ashvin Vishwanath, “Structure and topology of band structures in the 1651 magnetic space groups,” *Sci. Adv.* **4**, eaat8685 (2018).
- [24] Hoi Chun Po, “Symmetry indicators of band topology,” *J. Phys.: Condens. Matter* **32**, 263001 (2020).
- [25] Liang Fu and C. L. Kane, “Topological insulators with inversion symmetry,” *Phys. Rev. B* **76**, 045302 (2007).
- [26] Zhida Song, Tiantian Zhang, Zhong Fang, and Chen Fang, “Quantitative mappings between symmetry and topology in solids,” *Nature Commun.* **9**, 3530 (2018).
- [27] Tiantian Zhang, Yi Jiang, Zhida Song, He Huang, Yuqing He, Zhong Fang, Hongming Weng, and Chen Fang, “Catalogue of topological electronic materials,” *Nature* **566**, 475–479 (2019).
- [28] M. G. Vergniory, L. Elcoro, Claudia Felser, Nicolas Regnault, B. Andrei Bernevig, and Zhijun Wang, “A complete catalogue of high-quality topological materials,” *Nature* **566**, 480–485 (2019).
- [29] Feng Tang, Hoi Chun Po, Ashvin Vishwanath, and Xiangang Wan, “Comprehensive search for topological materials using symmetry indicators,” *Nature* **566**, 486–489 (2019).
- [30] Feng Tang, Hoi Chun Po, Ashvin Vishwanath, and Xiangang Wan, “Efficient topological materials discovery using symmetry indicators,” *Nature Phys.* **15**, 470–476 (2019).
- [31] Yuanfeng Xu, Luis Elcoro, Zhi-Da Song, Benjamin J. Wieder, M. G. Vergniory, Nicolas Regnault, Yulin Chen, Claudia Felser, and B. Andrei Bernevig, “High-throughput calculations of magnetic topological materials,” *Nature* **586**, 702–707 (2020).
- [32] Maia G. Vergniory, Benjamin J. Wieder, Luis Elcoro, Stuart S. P. Parkin, Claudia Felser, B. Andrei Bernevig, and Nicolas Regnault, “All topological bands of all nonmagnetic stoichiometric materials,” *Science* **376**, eabg9094 (2022).
- [33] Nikolas Claussen, B. Andrei Bernevig, and Nicolas Regnault, “Detection of topological materials with machine learning,” *Phys. Rev. B* **101**, 245117 (2020).
- [34] Guohua Cao, Runhai Ouyang, Luca M. Ghiringhelli, Matthias Scheffler, Huijun Liu, Christian Carbogno, and Zhenyu Zhang, “Artificial intelligence for high-throughput discovery of topological insulators: The example of alloyed tetradymites,” *Phys. Rev. Mater.* **4**, 034204 (2020).
- [35] Hang Liu, Sheng Meng, and Feng Liu, “Screening two-dimensional materials with topological flat bands,” *Phys. Rev. Materials* **5**, 084203 (2021).
- [36] Gabriel R. Schleder, Bruno Focassio, and Adalberto Fazzio, “Machine learning for materials discovery: Two-dimensional topological insulators,” *Appl. Phys. Rev.* **8**, 031409 (2021).
- [37] Nina Andrejevic, Jovana Andrejevic, B. Andrei Bernevig, Nicolas Regnault, Fei Han, Gilberto Fabbris, Thanh Nguyen, Nathan C. Drucker, Chris H. Rycroft, and Mingda Li, “Machine-learning spectral indicators of topology,” *Adv. Mater.* **34**, 2204113 (2022).
- [38] Andrew Ma, Yang Zhang, Thomas Christensen, Hoi Chun Po, Li Jing, Liang Fu, and Marin Soljačić, “Topogivity: A machine-learned chemical rule for discovering topological materials,” *Nano Lett.* **23**, 772–778 (2023).
- [39] Yi Zhang and Eun-Ah Kim, “Quantum loop topography for machine learning,” *Phys. Rev. Lett.* **118**, 216401 (2017).
- [40] Pengfei Zhang, Huitao Shen, and Hui Zhai, “Machine learning topological invariants with neural networks,” *Phys. Rev. Lett.* **120**, 066401 (2018).
- [41] Mathias S. Scheurer and Robert-Jan Slager, “Unsupervised machine learning and band topology,” *Phys. Rev. Lett.* **124**, 226401 (2020).
- [42] Nitesh Kumar, Satya N. Guin, Kaustuv Manna, Chandra Shekhar, and Claudia Felser, “Topological quantum materials from the viewpoint of chemistry,” *Chem. Rev.* **121**, 2780–2815 (2021).
- [43] Leslie M. Schoop, Florian Pielnhofer, and Bettina V. Lotsch, “Chemical principles of topological semimetals,” *Chem. Mater.* **30**, 3155–3176 (2018).
- [44] Xin Gui, Ivo Pletikoscic, Huibo Cao, Hung-Ju Tien, Xitong Xu, Ruidan Zhong, Guangqiang Wang, Tay-Rong Chang, Shuang Jia, Tonica Valla, Weiwei Xie, and Robert J. Cava, “A new magnetic topological quantum material candidate by design,” *ACS Cent. Sci.* **5**, 900–910 (2019).
- [45] B. Andrei Bernevig, Claudia Felser, and Haim Beidenkopf, “Progress and prospects in magnetic topological materials,” *Nature* **603**, 41–51 (2022).
- [46] Dongqin Zhang, Minji Shi, Tongshuai Zhu, Dingyu Xing, Haijun Zhang, and Jing Wang, “Topological axion states in the magnetic insulator  $\text{mnbi}_2\text{te}_4$  with the quantized magnetoelectric effect,” *Phys. Rev. Lett.* **122**, 206401 (2019).
- [47] Jiaheng Li, Yang Li, Shiqiao Du, Zun Wang, Bing-Lin Gu, Shou-Cheng Zhang, Ke He, Wenhui Duan, and Yong Xu, “Intrinsic magnetic topological insulators in van der waals layered  $\text{mnbi}_2\text{te}_4$ -family materials,” *Sci. Adv.* **5**, eaaw5685 (2019).
- [48] M. M. Otrokov, I. P. Rusinov, M. Blanco-Rey, M. Hoffmann, A. Yu. Vyazovskaya, S. V. Ereemeev, A. Ernst, P. M. Echenique, A. Arnau, and E. V. Chulkov, “Unique thickness-dependent properties of the van der waals interlayer antiferromagnet  $\text{mnbi}_2\text{te}_4$  films,” *Phys. Rev. Lett.* **122**, 107202 (2019).
- [49] Yue Li, Yadong Jiang, Jinlong Zhang, Zhaochen Liu, Zhongqin Yang, and Jing Wang, “Intrinsic topological phases in  $\text{mn}_2\text{bi}_2\text{te}_5$  tuned by the layer magnetization,” *Phys. Rev. B* **102**, 121107(R) (2020).
- [50] Hongyi Sun, Bowen Xia, Zhongjia Chen, Yingjie Zhang, Pengfei Liu, Qiushi Yao, Hong Tang, Yujun Zhao, Hu Xu, and Qihang Liu, “Rational design principles of the quantum anomalous hall effect in superlattice-like magnetic topological insulators,” *Phys. Rev. Lett.* **123**, 096401 (2019).
- [51] Yang Li, Jiaheng Li, Yang Li, Meng Ye, Fawei Zheng, Zetao Zhang, Jingheng Fu, Wenhui Duan, and Yong Xu,

- “High-temperature quantum anomalous hall insulators in lithium-decorated iron-based superconductor materials,” *Phys. Rev. Lett.* **125**, 086401 (2020).
- [52] Qilong Sun, Yandong Ma, and Nicholas Kioussis, “Two-dimensional dirac spin-gapless semiconductors with tunable perpendicular magnetic anisotropy and a robust quantum anomalous hall effect,” *Mater. Horiz.* **7**, 2071–2077 (2020).
- [53] X. Xuan, Z. Zhang, C. Chen, and W. Guo, “Robust quantum anomalous hall states in monolayer and few-layer tite,” *Nano Lett.* **22**, 5379–5384 (2022).
- [54] Yadong Jiang, Huan Wang, and Jing Wang, “Large-gap quantum anomalous hall insulators in the  $a\text{Ti}x$  ( $a = \text{K}, \text{rb}, \text{sr}; x = \text{sb}, \text{bi}, \text{sn}$ ) class of compounds,” *Phys. Rev. B* **108**, 165122 (2023).
- [55] Kapildeb Dolui, Sujay Ray, and Tanmoy Das, “Intrinsic large gap quantum anomalous hall insulators in  $\text{La}x(x = \text{Br}, \text{Cl}, \text{I})$ ,” *Phys. Rev. B* **92**, 205133 (2015).
- [56] Zhao Liu, Gan Zhao, Bing Liu, Z. F. Wang, Jinlong Yang, and Feng Liu, “Intrinsic quantum anomalous hall effect with in-plane magnetization: Searching rule and material prediction,” *Phys. Rev. Lett.* **121**, 246401 (2018).
- [57] Junjie He, Xiao Li, Pengbo Lyu, and Petr Nachtigall, “Near-room-temperature chern insulator and dirac spin-gapless semiconductor: nickel chloride monolayer,” *Nanoscale* **9**, 2246–2252 (2017).
- [58] Qilong Sun and Nicholas Kioussis, “Prediction of manganese trihalides as two-dimensional dirac half-metals,” *Phys. Rev. B* **97**, 094408 (2018).
- [59] Jing-Yang You, Zhen Zhang, Bo Gu, and Gang Su, “Two-dimensional room-temperature ferromagnetic semiconductors with quantum anomalous hall effect,” *Phys. Rev. Applied* **12**, 024063 (2019).
- [60] Jiaxiang Sun, Xin Zhong, Wenwen Cui, Jingming Shi, Jian Hao, Meiling Xu, and Yinwei Li, “The intrinsic magnetism, quantum anomalous hall effect and curie temperature in 2d transition metal trihalides,” *Phys. Chem. Chem. Phys.* **22**, 2429–2436 (2020).
- [61] Zeyu Li, Yulei Han, and Zhenhua Qiao, “Large-gap quantum anomalous hall effect in monolayer halide perovskite,” *Phys. Rev. B* **104**, 205401 (2021).
- [62] Zeyu Li, Yulei Han, and Zhenhua Qiao, “Chern number tunable quantum anomalous hall effect in monolayer transitional metal oxides via manipulating magnetization orientation,” *Phys. Rev. Lett.* **129**, 036801 (2022).
- [63] Kamal Choudhary, Kevin F. Garrity, Jie Jiang, Ruth Pachter, and Francesca Tavazza, “Computational search for magnetic and non-magnetic 2d topological materials using unified spin-orbit spillage screening,” *npj Comput. Mater.* **6**, 49 (2020).
- [64] Jun Zhou, Lei Shen, Miguel Dias Costa, Kristin A. Persson, Shyue Ping Ong, Patrick Huck, Yunhao Lu, Xiaoyang Ma, Yiming Chen, Hanmei Tang, and Yuan Ping Feng, “2dmatpedia, an open computational database of two-dimensional materials from top-down and bottom-up approaches,” *Sci. Data* **6**, 86 (2019).
- [65] G. Kresse and J. Furthmüller, “Efficient iterative schemes for ab initio total-energy calculations using a plane-wave basis set,” *Phys. Rev. B* **54**, 11169–11186 (1996).
- [66] See Supplemental Material for methods and technical details.
- [67] Yan Gong, Jingwen Guo, Jiaheng Li, Kejing Zhu, Menghan Liao, Xiaozhi Liu, Qinghua Zhang, Lin Gu, Lin Tang, Xiao Feng, Ding Zhang, Wei Li, Canli Song, Lili Wang, Pu Yu, Xi Chen, Yayu Wang, Hong Yao, Wenhui Duan, Yong Xu, Shou-Cheng Zhang, Xucun Ma, Qi-Kun Xue, and Ke He, “Experimental realization of an intrinsic magnetic topological insulator,” *Chin. Phys. Lett.* **36**, 076801 (2019).
- [68] Mikhail M. Otrokov, Ilya I. Klimovskikh, Hendrik Bentmann, Alexander Zeugner, Ziya S. Aliev, Sebastian Gass, Anja U. B. Wolter, Alexand ra V. Koroleva, Dmitry Estyunin, Alexander M. Shikin, Maria Blanco-Rey, Martin Hoffmann, Alexand ra Yu. Vyazovskaya, Sergey V. Ereemeev, Yury M. Koroteev, Imamaddin R. Amiraslanov, Mahammad B. Babanly, Nazim T. Mamedov, Nadir A. Abdullayev, Vladimir N. Zverev, Bernd Büchner, Eike F. Schwier, Shiv Kumar, Akio Kimura, Luca Petaccia, Giovanni Di Santo, Raphael C. Vidal, Sonja Schatz, Katharina Kifner, Chul-Hee Min, Simon K. Moser, Thiago R. F. Peixoto, Friedrich Reinert, Arthur Ernst, Pedro M. Echenique, Anna Isaeva, and Evgueni V. Chulkov, “Prediction and observation of an antiferromagnetic topological insulator,” *Nature* **576**, 416–422 (2019).
- [69] Si Li, Ying Liu, Zhi-Ming Yu, Yalong Jiao, Shan Guan, Xian-Lei Sheng, Yugui Yao, and Shengyuan A. Yang, “Two-dimensional antiferromagnetic dirac fermions in monolayer  $\text{taCoTe}_2$ ,” *Phys. Rev. B* **100**, 205102 (2019).
- [70] Federico Mazzola, Barun Ghosh, Jun Fujii, Gokul Acharya, Debashis Mondal, Giorgio Rossi, Arun Bansil, Daniel Farias, Jin Hu, Amit Agarwal, Antonio Politano, and Ivana Vobornik, “Discovery of a magnetic dirac system with a large intrinsic nonlinear hall effect,” *Nano Lett.* **23**, 902–907 (2023).
- [71] F. Ersan, H. D. Ozaydin, and O. Üzengi Aktürk, “Stable monolayer of the  $\text{ruo}_2$  structure by the peierls distortion,” *Philos. Mag.* **99**, 376–385 (2018).
- [72] Dong-Su Ko, Woo-Jin Lee, Soohwan Sul, Changhoon Jung, Dong-Jin Yun, Hee-Goo Kim, Won-Joon Son, Jae Gwan Chung, Doh Won Jung, Se Yun Kim, Jeongmin Kim, Wooyoung Lee, Chan Kwak, Jai Kwang Shin, Jung-Hwa Kim, and Jong Wook Roh, “Understanding the structural, electrical, and optical properties of monolayer h-phase  $\text{ruo}_2$  nanosheets: a combined experimental and computational study,” *NPG Asia Mater.* **10**, 266–276 (2018).